

# EXPERIMENTAL SET UP FOR MEASURING ONSHORE AND ONBOARD PERFORMANCES OF LEADING EDGE INFLATABLE KITES - PRESENTATION OF ONSHORE RESULTS

**M. Behrel**, ENSTA Bretagne, France, morgan.behrel@ensta-bretagne.org

**K. Roncin**, ENSTA Bretagne, France, kostia.roncin@ensta-bretagne.fr

**J.-B. Leroux**, ENSTA Bretagne, France, jean-baptiste.leroux@ensta-bretagne.fr

**F. Montel**, ENSTA Bretagne, France, frederic.montel@ensta-bretagne.fr

**A. Nême**, ENSTA Bretagne, France, alain.neme@ensta-bretagne.fr

**C. Jochum**, ENSTA Bretagne, France, christian.jochum@ensta-bretagne.fr

**Y. Parlier**, beyond the sea, France, yves.parlier@beyond-the-sea.com

This paper describes an experimental set up aiming to control and measure performances of small leading edge inflatable kite (lower than 12m<sup>2</sup>). This set up can be deployed onshore or on a dedicated boat. Two experimental campaigns were achieved using this set-up, one onshore in June 2016, and the second one at sea on April 2017. This paper focuses on the first one, and after a detailed presentation of sensors, it presents an specific post processing of the data including phase averaging. The guideline of this work is to estimate the variation of the lift coefficient and lift to drag ratio along 8-pattern trajectories. Results show a loss of lift coefficient of about 20% of the maximum value during kite turn. The lift to drag ratio evolution along a trajectory is also going through a local minima during kite turn (even if global evolution is questionable and still need further work). Nevertheless these trends still require the post processing of the whole experimental database, in order to be confirmed and properly interpreted

## NOMENCLATURE

|                      |  |       |
|----------------------|--|-------|
| $\underline{F}_k$    | Kite force vector measured by the 3D load cell | (N)   |
| $\underline{P}_k$    | Kite position vector                           | (m)   |
| $\underline{V}_a$    | Apparent wind velocity vector at kite position | (m/s) |
| $\underline{V}_k$    | Kite velocity vector                           | (m/s) |
| $\underline{V}_{TW}$ | True wind velocity vector at kite position     | (m/s) |
| $L_t$                | Tether length                                  | (m)   |
| $R_a$                | Aerodynamic Reference Frame                    | (-)   |
| $R_{TW}$             | Average True Wind Reference Frame              | (-)   |

## 1 INTRODUCTION

With the current continual growth of the global maritime traffic, finding ways to decrease environmental footprint without higher costs has become a real objective. In this context, French offshore sailor Yves Parlier has set up an innovating project aiming to develop the use of large kites as auxiliary propulsion device for ships, ranging from small pleasure boats to very large container vessels. The graduate and post graduate school of engineering ENSTA Bretagne - IRDL has been chosen to support the project, and several research actions have been started [1]. One of them aims to provide experimental data to benchmark and validate numerical models developed in the laboratory. A few research groups have already undergone trials and measurements on kite, mainly on

shore, like Dadd [2] or Fagiano [3], and frequently with an electricity production objective [4]. Sea trials and measurements have only been conducted by the SkySails team [5].

In the objective of acquiring experimental data, the development of an experimental set up for measuring kite performances onshore and on board have been done. Two experimental campaigns were carried out, the first one held onshore in June 2016, and the second held on board in April 2017 on a dedicated 6-meter-long boat. After a presentation of the experimental set up, and a brief oversight of the boat used in April 2017, focus will be done on the exploitation of the results got onshore in June 2016. Many 8-pattern trajectories were recorded during this campaign, and a post processing including phase averaging have been developed, to compute lift coefficient and lift to drag ratio of the kite. The aim is to estimate the variation of these parameters depending on the the position of the kite along the trajectory. Indeed, previous works

using zero-mass model as presented by Leloup et al. [1] always use a constant value of these parameters along 8-pattern trajectories.

## 2 EXPERIMENTAL SET-UP

The experimental set-up used for this measurement campaign is based on a kite control box with sensors and actuators, and two additional boxes containing batteries and data acquisition



Figure 1: Picture of the KiteLab, the experimental platform specifically designed to carry out measurements on effects and performances of kite propulsion. The 5-meter wind measurement mast is visible on the rear of the boat. The inflatable kite flying over the boat is a 5m<sup>2</sup> one.

and control system. This trio can be deployed onshore, fixing the kite control box into the ground (Fig. 2), or on board, embedding the system on the boat specifically designed for this purpose (Fig. 1). The kite used for this study is a Cabrinha Switchblade®, with an area of 5 square meters, usually used by kite surfers for leisure sport. Other kites have been tested on the kiteboat. This kite has four tethers, two on each side of the kite: the first two are called front tethers, and have constant length. The two others, called back tethers, have variable length and are used for control purpose. Various lengths of tethers were tested during trials, from 25 meters to 80 meters.

## 2.1 MAIN SENSORS

### 2.1.1 Forces Measurements

The major sensor of the experimental device is a three dimensional load cell, providing intensity and direction of the force into the front tethers. The load cell is a TR3D-B-1K built by Michigan Scientific, with a range on each axis of 1,000 pounds (4,448 N), and a safe overload of 300% of the full scale. This product is similar to the one used on a previous study [6], but with a smaller range of measurement suitable for forces generated by a 5m<sup>2</sup> kite. This sensor has a non-linearity error specified by manufacturer as being under 0.5% of full scale, and hysteresis and repeatability errors under 0.05% of full scale each. A complete calibration of the measurement chain was not carried out before the trials, and sensibilities provided by manufacturer have been used. However a calibration control set-up is under development, using test machines available at ENSTA Bretagne's laboratory, and

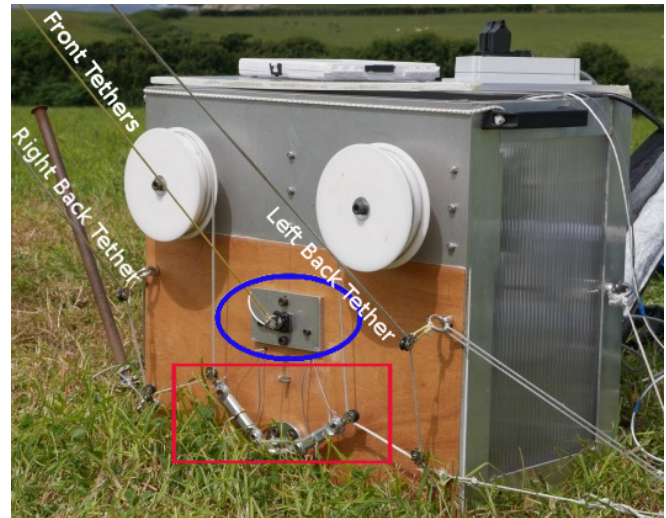


Figure 2: Kite control and measurement device deployed on shore. The two winches are visible, as well as the 3D front tether load cell (blue ellipse) and the two 1D back tether load cells (red rectangle).

the sensitivity and accuracy of the sensor will be compared with manufacturer ones.

For back tethers, due to their variable lengths, another measurement system must be used. This one is based on two simple load cells (Futek LCM200) measuring forces after a return pulley. These load cells have a full scale load of 4,500 N, with a specified non-linearity error under 0.5% of full scale, an hysteresis error under 0.5% of full scale and repeatability error under 0.1% of full scale. Various set-ups for return pulley have been tested, leading to various return angles. These angles were all the time carefully measured to be able to retrieve the real load in tethers.

### 2.1.2 Onshore Wind Measurements

Intensity and direction of the wind at kite altitude are important informations to get, in order to realize a valuable post processing, as it has been shown in previous work [6]. However with a kite flying between 10 and 80 meters above the ground, it is difficult to get a wind measurement with a good accuracy at any position of the kite. To deal with this problem, it was decided to use a wind profiler, based on sonic technology (Fig. 3). This type of device is called SODAR, for SOnic and Detection And Ranging. In our case, the SODAR was able to measure a profile from 13 meters above the ground to 108 meters, with one point every 5 meters, and averaging data over a 5-minute-period. For each point of measurement, the direction, the intensity and the vertical component were available, but also the standard deviations for each data. It was particularly important to have a wind profiler for these onshore measurements because of the topographic configuration of the field where the trials were carried out. Indeed, it has been observed some variations of the intensity and/or direction and/or vertical intensity of the wind along the altitude that could not have been easy to model.

To catch higher rate wind variation, an ultrasonic three di-



Figure 3: The SODAR (SONic and Detection And Ranging) device used for the onshore kite measurements.

mensional anemometer METEK USA-1 was also used. This anemometer was put in place on a mast at 8 meter above the ground, and had an acquisition rate of 20 hertz.

## 2.2 KITE CONTROL SYSTEM

### 2.2.1 Control And Data Acquisition System

All the control system and the data acquisition system is driven by a National Instruments compactRIO motherboard, with additionally I/O modules, ensuring that all the recorded data are sampled synchronously. These modules provides analog and digital inputs, serial ports, and full bridge analog inputs for load cells data acquisition. The whole system is completely programmed using the National Instruments software LabVIEW.

The kite can be steered by applying a difference between the back tether lengths. For this purpose, each back tether is attached to an electric winch, and the winches are controlled in position, thanks to optical encoders with an accuracy of 4096 counts per revolution. Thus, for a given differential set-point  $\delta$ , one winch shall shift by a value  $\delta/2$  and the other winch by a value of  $-\delta/2$ . Each winch has a power of 800 watt, and are able to roll in or roll out tethers at a speed of  $0.7 \text{ m.s}^{-1}$ . The maximum differential speed is then  $1.4 \text{ m.s}^{-1}$ . A power card interfaces the compactRIO and the winches.

### 2.2.2 Dynamic Flight Automatic Pilot

The winches can be controlled by 2 joysticks for a manual control of the kite, but an automatic pilot can be also engaged, enabling the steering of 8-pattern trajectories with good reproducibility. This autopilot is mainly based on Fagiano work [3]. To get a proper functioning of the autopilot, the kite position in the wind window has to be known at any time to ensure a feedback to the controller. More specifically, motions of the kite has to be known, because the kite is undergoing dynamic flight. That means that the kite position data shall be not too noisy to allow the computation of the first order time derivative process leading to the velocity (Eq. (2)). In our

case, the kite position is obtained thanks to the 3D load cell, assuming that front tethers are straight, their lengths having been carefully measured. To reduce noise level on position data, load cell acquisition is done at 10 kHz, and then the signal is averaged at a frequency of 200 Hz. After the derivative process, the derivative signal is filtered with a 40 ms running average filter.

## 2.3 KITEBOAT SPECIFIC SENSORS

In addition to the experimental setup already described in the previous part, sensors are added to get the specific measurements associated with a moving platform, namely the KiteLab boat at sea.

### 2.3.1 Inertial Measurement Unit (IMU)

An IMU combined with a two GPS receivers provides boat orientations and velocity. This sensor is VectorNav VN-300 Rugged. Thanks to the MEMs inertial sensors, associated to advanced Kalman filtering algorithms provided by manufacturer, the heel and pitch orientation can be obtained. Data from MEMs (angular rate and acceleration) are also recorded at any time. The two GPS receivers, in addition to provide position and velocity of the boat, give also an accurate heading measurement, apart from any magnetic disturbance. With this accurate measurement of heading, it becomes possible to estimate the drift of the boat, relatively to the ground, comparing heading of the boat and course over ground obtained from GPS receivers. The drift relatively to the sea water can be estimated taking into account currents. According to the specification sheet, the orientation static accuracies are under  $0.5^\circ$  RMS, and under  $0.3^\circ$  RMS in dynamic case. Velocity accuracy is  $0.05 \text{ m.s}^{-1}$ . It is planned for future work to benchmark the VN-300 with higher IMU grade.

### 2.3.2 Rudder Angle

A fully sealed linear potentiometer is set up into the steering system to get the rudder angle. This sensor was calibrated in the laboratory and the accuracy is lower than  $0.5^\circ$ .

### 2.3.3 Onboard Wind Measurements

As it has been recalled in part 2.1.2, wind estimation at kite altitude is one of the most important data required to get proper post processed data. However during sea trials, it is not possible to embedded the SODAR on board, due to insufficient room and technological issues (the SODAR needs to be set up in perfect horizontal position for a accurate measurements). Moreover, due to operational constraints, it was not relevant to set up a wind measurement mast higher than 5m. However wind gradient above the sea surface is less disturbed than onshore, and can be reasonably estimated using statistical formulas. To check the evolution of wind gradient, three sonic anemometers are fixed on the mast at three different elevations. This assembly provides also a redundancy of wind measurement. The three sonic anemometer are manufactured by Gill, but are different models. The higher one, with a

measurement altitude of 5.5m above the sea level is a WindMaster, a three dimensional anemometer, fixed on the head of the mast. The second one is a 2D anemometer WindSonic placed at 4.2m above the sea level and deported from the mast by 0.6m. The last anemometer is a MaxiMet 500. This is also a 2D anemometer, and combines wind measurements with pressure, temperature and relative humidity measurements. This sensor is also fitted with a GPS sensor and a compass, and can provide the velocity of the wind into axis system attached to the earth, corrected from the boat velocity. This measurement is redundant when the measurement mast is set up on the kiteboat. The MaxiMet is located at 3.0m above sea level, and is also deported from the mast by 0.6m (see Fig. 1).

The misalignment angles of the sensors with respect to the axis of the mast have been measured in laboratory, as well as the misalignment angle of the mast with respect to the longitudinal boat axis. Data werer corrected accordingly during post processing.

### 3 DATA POST PROCESSING

Only data coming from the experimental campaign carried out on shore in June 2016 have been post processed. Data acquired with the KiteLab during the experimental campaign carried out in April 2017 are still under process. Thus, following parts deal only with on shore data.

The aim of this post processing is to retrieve lift to drag ratio and lift coefficient of the kite, and to estimate the variation of these parameters along a trajectory. However, to calculate these values, wind at kite position needs to be known at any time and SODAR device was only able to provide average value of wind along altitude with a sampling period of 5min. To deal with this issue, it was decided to perform measurement runs of several minutes and to compute phase averaging on the recorded data.

#### 3.1 LIFT-COEFFICIENT AND LIFT-TO-DRAG RATIO

To get the lift coefficient and the lift to drag ratio, the apparent wind on the kite  $\underline{V}_a$  needs to be known. The latter is the difference between the relative wind velocity at kite altitude and the kite velocity  $\underline{V}_k$ . In our specific case of onshore measurement with no velocity of the ground station, relative wind is equal to true wind  $\underline{V}_{TW}$ . However true wind depends on altitude. The kite velocity can be obtained by computing the time derivative of the kite position  $\underline{P}_k$ , and kite position is obtained from the 3D load cell measurement, assuming front tethers are straight with constant lengths. Forces and positions vector are expressed into the Average True Wind Velocity reference frame  $R_{TW}$ , defined with the unit vector  $\underline{x}_{TW}$  obtained with the projection of the mean value of the true wind speed onto the horizontal plane. The unit vector  $\underline{z}_{TW}$  is then vertical pointing down, and the unit vector  $\underline{y}_{TW}$  is completing the coordinate system to create a direct axis system.

$$\underline{P}_k = \frac{\underline{F}_k}{\|\underline{F}_k\|} * L_t \quad (1)$$

$$\underline{V}_a = \underline{V}_{TW} - \underline{V}_k = \underline{V}_{TW} - \frac{d\underline{P}_k}{dt} \quad (2)$$

From there, it becomes possible to define an aerodynamic reference frame  $R_a$  with the unit vector  $\underline{x}_a$  parallel and opposite to the apparent wind velocity vector  $\underline{V}_a$  (and so parallel to the drag force), while the unit vector  $\underline{z}_a$  is parallel and opposite to the lift force of the kite. Thus, lift coefficient and lift to drag ratio can be obtained by Eq. (5) and (6).

$$\underline{D} = -(\underline{F}_k \cdot \underline{x}_a)\underline{x}_a \quad (3)$$

$$\underline{L} = \underline{F}_k - \underline{D} \quad (4)$$

$$\frac{L}{D} = \frac{\|\underline{L}\|}{\|\underline{D}\|} \quad (5)$$

$$C_l = \frac{\|\underline{L}\|}{\frac{1}{2}\rho A_k V_a^2} \quad (6)$$

#### 3.2 WIND ESTIMATION AT KITE POSITION

With the present experimental set up, wind were only measured at 2 locations close from each other, at 2 different frequencies. Thus it was not possible to catch wind variation into the horizontal plane. This leads to the hypothesis than the wind was uniform between the point of measurement and the kite horizontal position. Then, to deal with the low frequency of SODAR data, it has been decided to realize a basic linear temporal interpolation, coupled with a spatial linear interpolation for wind variation along the vertical axis. Metek data are not used in this case.

Other strategies can be considered, like the use of SODAR data to define an average wind profile, and the use of Metek data to catch higher frequency variation. However, the Metek measurements were probably really disturbed by ground proximity, and the result of such strategy seemed to be uncertain. Thus, the test of such a method was delayed to further work.

#### 3.3 PHASE AVERAGING

The autopilot described in section 2.2.2 is able to perform repeatable 8-pattern trajectories, as illustrated in Fig. 4. Nevertheless, due to the variability of the boundary conditions of such full scale outdoors experiments, small variations around a mean periodic trajectory are observed during measurements of several minutes. Therefore for the analysis of each runs, a phase averaging procedure of the recorded data [7] is applied in order to determine the mean trajectory and all the associated time sampled mean characteristics along it: environmental condition, kite control parameters and tensions of the tethers.

The chosen detection signal is the FY force, which is directly one of the three signals provided by the 3D load cells; each elementary 8-pattern trajectory being a specific pattern visible on this signal. In order to window the detection signal, its main frequency and then the period of the 8-pattern trajectory are first computed using the Fast Fourier Transform (FFT) algorithm of Matlab®. The detection signal is centered on 0 by subtracting to the signal its mean value. Then it is windowed with the following process: the first point of each window is found when the signal becomes positive and the widow

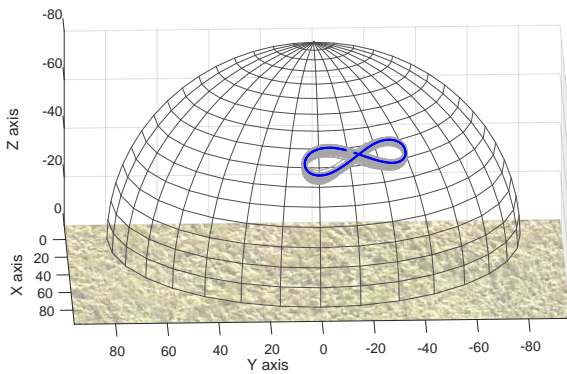


Figure 4: 5-square-meter kite trajectory (grey line) during a 10-minute record, with 80-meter tethers. The bold blue line shows the kite trajectory resulting from the phase averaging process. Kite positions are expressed in the Average True Wind reference frame  $R_{TW}$ .

length is set equal to the period of the trajectory. This leads to a set of elementary signals of equal lengths, each associated with one elementary 8-pattern trajectory of the run. A representative one of these elementary signal is chosen as the reference one, and the cross correlation of each window with that reference is finally calculated. This leads to a set of maximum correlation levels and set of small time shift for each window to reach this maximum, which are used to slightly correct the beginning of the corresponding windows. This whole process of the detection signal being achieved, all the simultaneously sampled signals recorded in the considered run can be windowed using the obtained final set of the starting and ending time index. Finally for each signals, for each sampled instant of the period, a mean value and a standard deviation value can be calculated from the set of corresponding values in each elementary window. Moreover, as the cross correlation process is returning a level of best correlation for each detected window, it is possible to remove corrupted patterns from the set. A limit has been defined to only keep windows for which detection patterns have a cross correlation level of 90% of the level of the auto correlation of the reference detection pattern. This limit leads to remove of about 30% of the number of periods recorded in a run.

Typical results of this windowing process is shown in Fig. 5 on two variables; the total force generated by the kite and the azimuth angle, with the associated standard deviations. Lift to drag ratio and lift coefficient can also be computed using Eq. 1 to Eq. 4. Results are presented in the next part.

#### 4 RESULTS

The presented results are related to 3 records done with 80-meter tethers, with various size of 8-pattern trajectories. All the runs were recorded during the same day, with a steady wind blowing from the sea and allowing a high repeatability rate of the trajectories, as it can be seen on Fig. 6. Runs are named from (a) to (c) by ascending order of trajectory size. On each case, the phase averaging process were computed as

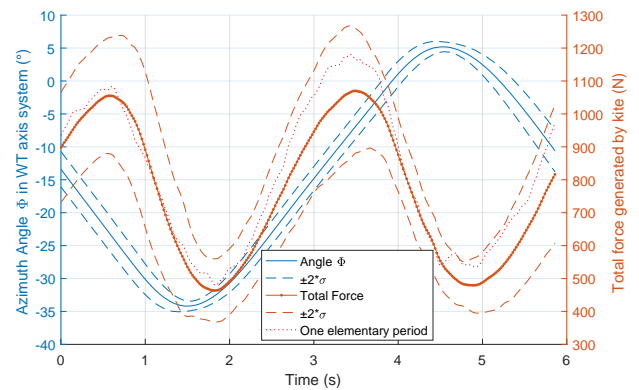


Figure 5: Evolution of the azimuth kite angle and the total force, and associated standard deviation along the average trajectory. One elementary period is also plotted for the total force.

presented in part 3.3. The proportion of trajectories matching the conditional parameter of 90% of the cross correlation are respectively, for case (a) to (c), 52%, 93% and 59%. These proportions lead to phase averaging process done respectively on 52 (10-minute run), 50 (8-minute run) and 26 (7-minute run) patterns.

#### 4.1 RAW RESULTS

Lift Coefficient and Lift to Drag ratio have been then computed for each of the 3 cases of Fig. 6. Each case corresponding to various sizes of the 8-pattern trajectory, period duration is different from a case to another. To compare the 3 cases, results are plotted with respect to a dimensionless time variable, get from the division of the time vector of the case by the period duration of the case. Results are shown in Fig. 7.

Because trajectories seem to be very symmetrical, we should expect to retrieve this particularity in the evolution of lift coefficient and lift to drag ratio along the trajectory. However, this is not really visible in Fig. 7. In fact trajectories and load along trajectories are very symmetrical regarding the center of the trajectories, however this center is not centered on the true wind axis (equal to the X-axis in Fig. 6). Consequently dissymmetrical outcomes are reported on lift coefficient and lift to drag ratio. This problem of symmetry has been noticed during measurement, but the reason was not identified with certainty. A few explanations are possible. The kite could be slightly dissymmetrical or left and right tethers had not exactly the same length. Kite geometry has been visually checked, but no evidence of differences between sides was found. A difference between left and right front tethers about 5cm was found after the trial (0.06% of the tether length). The hypothesis of an uniform wind for all points at the same altitude can be also questionned. Indeed with 80m tethers, 8-patterns are more than 50 meter large, and with the topographic configuration of the field, the kite could undergo different wind on the opposite sides of the pattern.

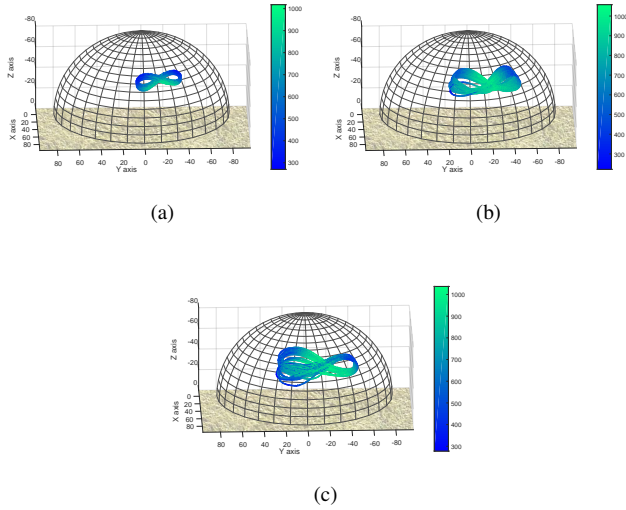


Figure 6: Kite trajectory record during the 3 measurement runs considered in this part (expressed into the Wind True axis system). The automatic pilot settings were modified between runs to generate various 8-pattern trajectory sizes. Thus the maximum amplitude on kite azimuth angle is  $40^\circ$  for case (a),  $60^\circ$  for case (b) and  $67^\circ$  for case (c).

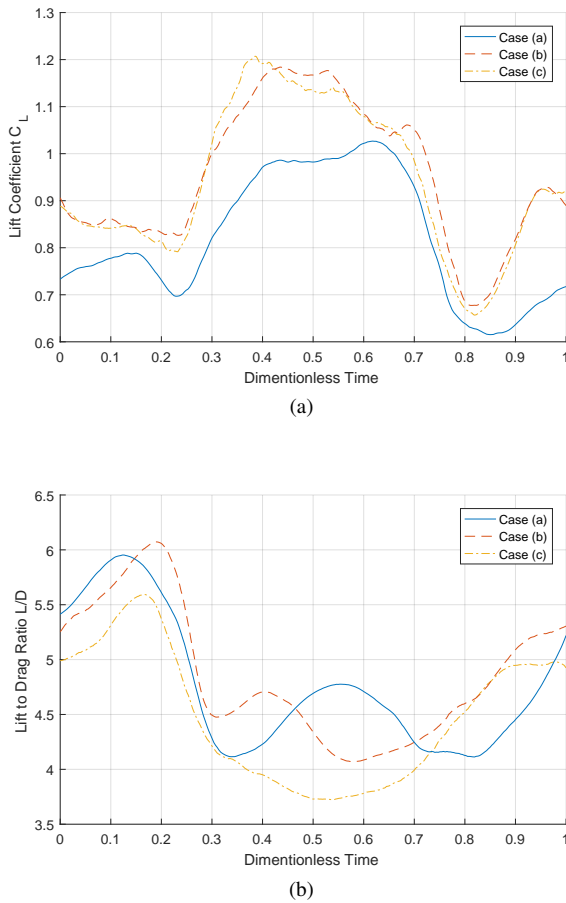


Figure 7: Evolution of the average Lift Coefficient (a) and average Lift To Drag ratio (b) of the kite along the average trajectory, for the 3 cases presented in Fig.6

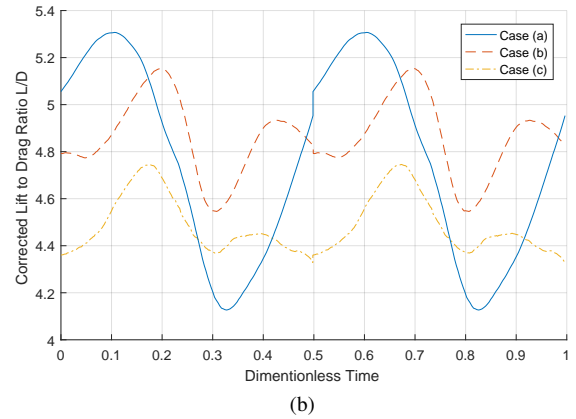
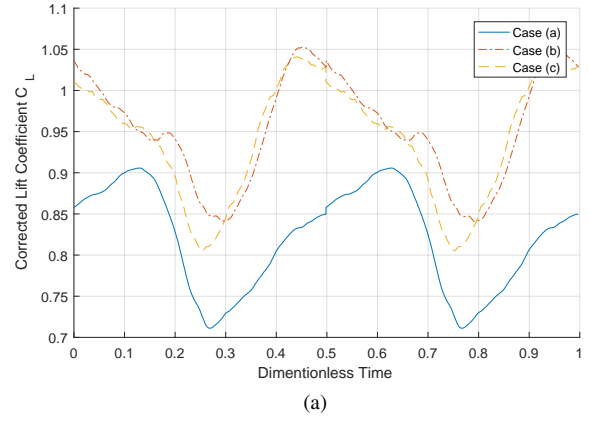


Figure 8: Evolution of the corrected average Lift Coefficient (a) and corrected average Lift To Drag ratio (b) of the kite along the average trajectory using Eq. (7).

#### 4.2 CORRECTED RESULTS

To deal with the problem of symmetry, and to analyze the evolution of the lift coefficient and lift to drag ratio of the kite depending on the rotation rate of the kite, it has been decided to make symmetrical these two signals. For this purpose, each signal has been cut into two pieces of equal length, and these two pieces have then been averaged. Thus, for a signal  $S$  defined for  $t \in \llbracket 0, \tau \rrbracket$ , the symmetrical signal  $S_{sym}$  is:

$$S_{sym}(t) = \begin{cases} \frac{S(t)+S(t+\frac{\tau}{2})}{2} & t \in \llbracket 0, \frac{\tau}{2} \rrbracket \\ \frac{S(t-\frac{\tau}{2})+S(t)}{2} & t \in \llbracket \frac{\tau}{2}, \tau \rrbracket \end{cases} \quad (7)$$

Equation (7) has been computed for lift coefficient and lift to drag ratio signals of the 3 cases. Results are shown in Fig. 8.

To provide a more accurate analyze of the evolution of the corrected lift coefficient along a trajectory, the latter has also been plotted in respect to the angle  $\gamma$  as defined by Fagiano in [3] (Fig. 9). This variable is the angle between the local meridian of the sphere passing through the kite position and the kite velocity vector. For instance if  $\gamma = 0^\circ$  the kite is moving upward toward the zenith of the sphere.

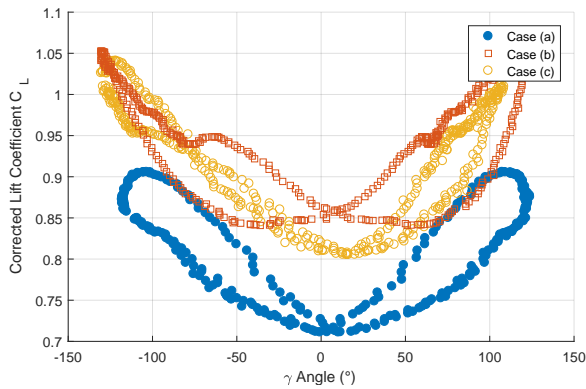


Figure 9: Lift Coefficient of the kite during the 3 considered cases in respect to  $\gamma$  angle.

## 5 DISCUSSION

Figure 8(a) shows a clear trend concerning the evolution of lift coefficient along the trajectory, with a drop of about 20% during the turn of the kite, with a minimum when kite velocity vector is pointing upward (see Fig. 9). This trend is visible on each of the 3 cases. A good correlation exist between case (b) and (c), however case (a) shows lower values than the others, and no explanation making sense has been found so far. Moreover values of lift coefficient seem to be higher than in previous studies. Indeed, Dadd study [2] also focusing on leading edge inflatable kite got a lift coefficient about 0.78, which is sensible by Behrel et al. [6], but for bigger kite (50m<sup>2</sup>).

For the lift to drag ratio, trends are less pronounced. Case (a) seems to follow to same rule than the lift coefficient with a drop synchronized with the drop on lift coefficient. For cases (b) and (c) it becomes more difficult to conclude, however a local minima can also be observed during kite turn (between 0.2 and 0.3 unit of dimensionless time, and between 0.7 and 0.8). Variations during straight part of the trajectory (between 0.4 and 0.6 unit of dimensionless time) could not have been explained for the moment. Medium values about 4.7 are this time sensible with [2] or [6]. However, all this process needs to be propagated over the numerous other runs that have been acquired during the days of this experimental campaign to get a more precise sight of these trends. That will be part of future works.

## 6 PERSPECTIVES

In addition to further analyses and developments that have been pointed out in the previous part, another important piece of work will be to study data obtained in April 2017 on the experimental boat Kitelab (see Fig. 1). This campaign was held in the bay of Quiberon with the support of the French National Sailing School (Ecole Nationale de Voile et des Sports Nautiques), especially Dr. Paul Iachkine. The navigation area was covered by 4 fixed wind measurement points, plus a chase boat also equipped with a wind measurement device. This wind measurement system would allow the reconstruction of

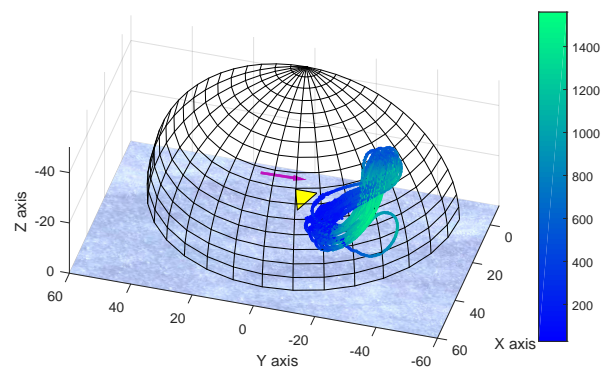


Figure 10: A 5-minute run with the KiteLab in the bay of Quiberon. The yellow triangle is for the boat, and the purple arrow is for the average true wind during the run. The bi-colorline is the track of the kite during the run, and the color scale accounts for the force generated by the kite.

the wind field (using spatial and temporal interpolation or micro meteorology model developed by a partner compagny). Runs with various kites, various tethers length, at different winds speed and directions were done. An example of raw results during such a run is given in Fig. 10. .

## 7 CONCLUSION

An kite experimental setup has been developed to be used onshore or embedded on board of a dedicated boat specifically developed. Load cells are used to get kite force and kite position into the wind window. Kite is controlled using winches, and an autopilot performs repeatable 8-pattern trajectories. During the onshore campaign held in June 2016, a sonic wind profiler was used to estimate the wind at kite position. A selected part of data obtained during this campaign has been post processed with a phase averaging method, leading to an estimation of loss of lift coefficient during turn of the kite.

Future work will focus on deeper analyzes of onshore kite measurements, as only a small part were used for the present study. Onboard data will be also post processed, using as often as possible the phase averaging process presented here.

## 8 ACKNOWLEDGEMENTS

The authors are grateful to the French agency for energy development and control (ADEME) for the funding of this study.

## REFERENCES

- [1] R. Leloup, K. Roncin, M. Behrel, G. Bles, J.-B. Leroux, C. Jochum, and Y. Parlier, "A continuous and analytical modeling for kites as auxiliary propulsion devoted to merchant ships , including fuel saving estimation," *Renewable Energy*, vol. 86, pp. 483–496, 2016. [Online]. Available: <http://dx.doi.org/10.1016/j.renene.2015.08.036>

- [2] G. M. Dadd, "Kite Dynamics for Ship Propulsion," Ph.D. dissertation, University of Southampton, 2012.
- [3] L. Fagian, a. U. Zraggen, M. Khammash, and M. Morari, "Automatic Crosswind Flight of Tethered Wings for Airborne Wind Energy: Modeling, Control Design, and Experimental Results," *IEEE Transactions on Control Systems Technology*, vol. 22, no. 4, pp. 1433–1447, 2014.
- [4] A. Bormann, M. Ranneberg, P. Kövesdi, C. Gebhard, and S. Skutnik, "Development of a Three-Line Ground-Actuated Airborne Wind Energy Converter," in *Airborne Wind Energy*, U. Ahrens, M. Diehl, and R. Schmehl, Eds. Berlin, Heidelberg: Springer Berlin Heidelberg, 2013, ch. 24, pp. 427–441.
- [5] M. Erhard and H. Strauch, "Control of Towing Kites for Seagoing Vessels," pp. 1–12, 2012.
- [6] M. Behrel, K. Roncin, D. Grelon, F. Montel, A. Nême, J.-B. Leroux, C. Jochum, and Y. Parlier, "Presentation of an experimental campaign for measuring performances and effects of a 50-square-meter kite put on a 13-meter trawler," in *15ème Journées de l'Hydrodynamique*, Brest, 2016.
- [7] P. Wernert and D. Favier, "Considerations about the phase averaging method with application to ELDV and PIV measurements over pitching airfoils," *Experiments in Fluids*, vol. 27, pp. 473–483, 1999.

## 9 AUTHORS BIOGRAPHY

**M. Behrel** is currently following a Ph.D. Degree at the Dupuy de Lôme Research Institute at the graduate and post graduate school of engineering, Ecole Nationale Supérieure de Techniques Avancées Bretagne (ENSTA Bretagne), Brest, Brittany, France. He graduated at ENSTA Bretagne in 2014 in naval architecture and offshore engineering.

**K. Roncin** is Associate Professor of Naval Hydrodynamics at the graduate and post graduate school of engineering, Ecole Nationale Supérieure de Techniques Avancées Bretagne (ENSTA Bretagne), Brest, Brittany, France. He is currently the head of the Master of Science in Naval Hydrodynamics and gave during several years specialized lectures in naval construction and design. He received his Ph.D. degree (2000) with Honours from the University of Nantes, France. His research skills cover seakeeping, manoeuvrability and sail yacht dynamics.

**J. B. Leroux** is Associate Professor of Naval Hydrodynamics at the graduate and post graduate school of engineering, Ecole Nationale Supérieure de Techniques Avancées Bretagne (ENSTA Bretagne), Brest, Brittany, France. He is currently in charge of fluid mechanics courses. He received his Ph.D. degree (2003) with Honours from the Ecole Centrale de Nantes and from the University of Nantes jointly, France. His research skills mainly cover hydrodynamics and cavitation of lifting bodies.

**A. Nême** is Associate Professor of Engineering and Materials Science at the graduate and post graduate school of engineering, Ecole Nationale Supérieure de Techniques Avancées Bretagne (ENSTA Bretagne), Brest, Brittany, France. He is currently in charge of mathematics and strength of materials courses. He received his Ph.D. degree (1994) with Honours from the Ecole Normale Supérieure de Cachan, France. His research skills mainly cover linear and non-linear analysis in structural engineering.

**C. Jochum** is Associate Professor of Mechanical Engineering and Materials Science at the graduate and post graduate school of engineering, Ecole Nationale Supérieure de Techniques Avancées Bretagne (ENSTA Bretagne), Brest, Brittany, France. He worked several years in the Industry as head of the research department for a French supplier of track maintenance and construction equipment, involved in rigid body mechanics and structures design. He received his Ph.D. degree (1999) with Honours from the University of Metz, Lorraine, France. His research skills cover thermosetting composites from multiphysics couplings and internal stress issues to dynamical behaviour and strengthening.

**Y. Parlier** has succeeded brilliantly in all the major nautical races and has strived throughout his life to promote respect for man and the environment. He has a graduate degree in composite materials and launched several innovations in sail yacht design. We remember the Vendée Globe 2000 when all alone, near an island of New Zealand, he successfully rebuilt and erected a new mast and finished his round the world voyage. Taking advantage of wind energy by using kites as auxiliary propulsion device is the aim of the "Beyond the sea" project launched by Yves Parlier.